

Using remote sensing to identify individual tree species in orchards: A review^{☆,☆☆}



Asli OZDARICI-OK^{a,*}, Ali Ozgun OK^b

^a Academy of Land Registry and Cadastre, Ankara Haci Bayram Veli University, Ankara, Türkiye

^b Dept. of Geomatics Engineering, Hacettepe University, Ankara, Türkiye

ARTICLE INFO

Keywords:

Fruit trees
Climatic zones
Orchards
Remote sensing
Image analysis
Machine learning
Deep learning
Tree identification
Crown delineation

ABSTRACT

Fruit trees are an essential subset of all tree species due to their high water and nutrient content. They play a vital role in human nutrition and provide a significant economic boost for top pomiculture countries. The purpose of this article was to investigate the published articles based on the categorization of orchard trees in accordance with the various climatic zones and conduct a review related to the methods for the identification of individual fruit trees in orchards. The review looked into the methods that have been used in the past to identify orchard trees and define the crowns of those trees. We highlight 74 articles that were published in 22 different journals published in the Web of Science database. A wide variety of conventional and modern digital image analysis techniques, including deep learning techniques, can be used to facilitate the efficient utilization of products derived from space-borne, airborne, and terrestrial systems. We believe that efficient orchard management to support consistent and sufficient fruit yields is a goal that should be prioritized. In this respect, fruit tree identification and modeling procedures are continually being enhanced and expanded thanks to ongoing research and development efforts. In this context, this review provides a detailed overview of the key aspects of the major efforts proposed for identifying individual fruit trees in orchards.

1. Introduction

Since the early 1960s, the population of the world has increased at a rapid rate, with high birth rates being recorded in South Asia and Sub-Saharan Africa. Because this trend and moving from rural to urban areas continues, it is more important than ever to make effective use of agricultural land that is being actively farmed (FAO, 2019). Trees are among the most important components of an ecosystem, not only because of their importance to agriculture but also because of their role in maintaining and regulating climate: improved water and air quality, as well as increased food security, forestry, shelter, and biodiversity, are all benefits.

If we consider the importance of providing fresh fruits to all kinds of people, it becomes clear that fruit trees are a particularly important subset of all tree species. Due to their high nutritional value and water content, fruits serve an essential function in human nutrition. Furthermore, the economic contribution of fruit trees is critical for the world's leading pomiculture countries. As a direct consequence, one of the most

crucial components of precision agriculture is not only locating tree groupings but also determining the crown diameter, shape, and size of individual fruit trees. The trunk position, crown closure, biomass, volume, and tree species are also important factors to consider (Kia, 2019). One of the most effective ways to collect data on the (bio)physical characteristics of individual trees and tree cover is through remote sensing science. Remote sensing and (photogrammetric) computer vision approaches are increasingly being used to generate the datasets required by the horticulture industry due to a lack of complete information recorded from fruit trees through more conventional means such as ground surveying. The reason for this is that remote sensing technology may provide timely, reliable, and accurate data on fruit tree structures and coverage.

In recent years, the availability of a wide variety of remotely sensed datasets like panchromatic and multispectral optical aerial and/or satellite images, synthetic aperture radar (SAR), light detection and ranging (LiDAR), hyperspectral, and thermal data of suitable quality has allowed to produce more accurate maps through the application of

* Web 1. <https://insightsimaging.springeropen.com/articles/10.1007/s13244-018-0639-9>** Web 2. <https://www.freepik.com>

* Corresponding author at: Academy of Land Registry, Ankara Haci Bayram Veli University, Emniyet District Abant street, No:10/2 06500 Yenimahalle, Ankara, Türkiye.

E-mail addresses: asli.ok@hbv.edu.tr (A. OZDARICI-OK), ozgunok@hacettepe.edu.tr (A.O. OK).

automated methods/approaches to determining the physical parameters of fruit trees (Ozdarici-Ok, 2015). Multiple platforms with distinct properties could be used to achieve the desired coverage and reliability. Terrestrial platforms are one of the most important components, with exceptional positional accuracy and a very high ground sampling distance (i.e., GSD up to mm). The most significant drawbacks of such systems are the length of time they take and the difficulties that may be encountered in reaching certain locations. An unmanned aircraft system (UAS), on the other hand, is economical in terms of cost and operating requirements up to a certain area coverage, and they are capable of delivering images with a high-resolution GSD (i.e., up to cm) and providing high positional accuracy. However, similar to manned aircraft platforms, they are susceptible to flying conditions that are unfavorable to their operation. Human-operated airborne systems have certain advantages over UAS, including greater area coverage, better image quality, and the ability to carry enhanced payloads that may access a broader spectrum of wavelengths. Another category of platform with the possibility of extensive coverage and a broad spectral range is earth-observing satellites. One of the limitations of satellite platforms is that their optical wavelengths are potentially subject to cloud cover and have a relatively lower GSD than other systems (Pádua et al., 2017) (Fig. 1).

Most studies on (fruit) trees that utilize the datasets collected through the aforementioned technologies divide individual tree identification process into two main tasks: (i) identification of trunk location of trees, and (ii) delineation of tree crowns. The research into tree identification typically focuses on identifying treetops, while tree crown delineation involves drawing the contour borders of tree crowns (Ke and Quackenbush 2011). Tree recognition (counting) in orchards and the delineation of urban tree crowns from high-resolution images were previously discussed in Gomes and Maillard (2016). They covered six fundamental state-of-the-art methods used for those main tasks: *local maxima filtering*, *template matching*, *valley following*, *watershed segmentation*, *region growing*, and *marked point process*.

In high-resolution images, the pixels at the top of the crowns of trees have the highest brightness value, and the values decrease as they move

toward the crown boundary. This is the key assumption of the *local maxima filtering* theory, and this assumption is noticeable in the majority of the tree species. The local maxima filtering makes use of the kernel search window in order to locate brightness pixel values within the kernel that are representative of tree crown pixels (Fig. 2a,b). However, the local maxima filter has the drawback of being insensitive to trees of varying crown diameters due to the use of a fixed-size window. Therefore, variable-size windows based on crown sizes are used to minimize this restriction. The method known as *template matching* is a technique for finding objects that involves making a correlation between the template of the object of interest and the image objects that are being analyzed. If there is a high degree of compatibility between the object being searched for and the model, then the object is found (Fig. 2c,d). Template matching suffers from the fundamental shortcoming of requiring a library for tree models in order to achieve the desired level of accuracy. Another strategy for identifying tree crowns as individuals or groups is the *valley following* algorithm. It employs shaded pixels between treetops and attempts to remove them from the brighter pixels indicating tree crowns. This aids in the separation of one tree crown from the other (Fig. 2e). This approach works best in situations with low sun elevation angles and conical tree formations. On the other hand, if tree diameters are very diverse, few trees exist, and the crown closure rate is significant, the output results will most likely be poor. *Watershed* is a method that uses image gradients rather than the image itself to determine watershed partitions of an image's topographic structure using predefined markers. It is a very basic image segmentation technique tailored to tree crown delineation, and it was combined with other techniques (such as local maxima) in the analyses (Fig. 2f). One major disadvantage of the watershed segmentation approach is that if the branches of trees are not compact, over segmentation may occur, affecting the output results. The *region growing* method uses seed pixels that are already established to search neighboring pixels for similar features, allowing it to distinguish between objects in an image (Fig. 2g). Successful application of the method is highly dependent on the degree of heterogeneity present in the input image. Another technique used for tree object recognition is the *marked point process* (MPP). It uses a

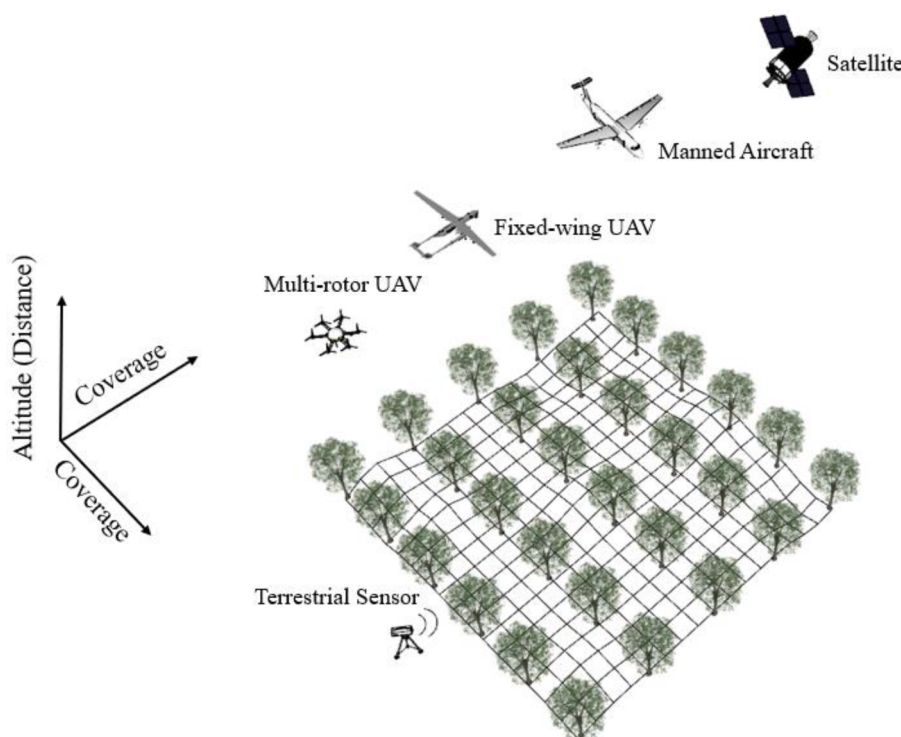


Fig. 1. Different remote sensing platforms utilized for the identification of fruit trees in orchards.

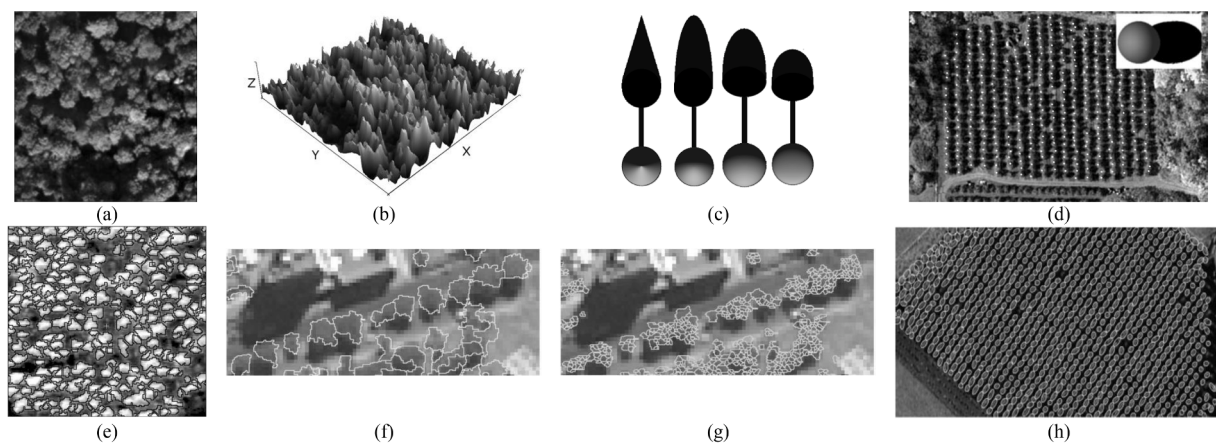


Fig. 2. Examples of surfaces resulting from the application of an LM kernel operator: (a) the original image, and (b) the local maxima in the third dimension are associated with the presence of trees, (c) examples of artificial tree models with various crown shapes. (d) apple orchard tree identification with the model used in the upper right corner, (e) results of applying valley-following to a Canadian forest image, (f) results of the watershed segmentation algorithm on a WorldView-2 image, (g) results of the region growing algorithm on a WorldView-2 image, (h) example of the use of MPP to identify tree crowns in a poplar plantation (source: [Gomes and Maillard, 2016](#)).

stochastic algorithm to search for objects in an image by comparing it to a predefined model and a set of marks. The algorithm may work well in a controlled setting with trees of similar age and size (Fig. 2h), but it is not suited to a more natural context involving complex settings. In addition to 2D tree structure delineation, template matching and marked point techniques can be employed for 3D tree object recognition ([Gomes and Maillard, 2016](#)).

In addition to the above-mentioned techniques, the individual trees can also be identified using especially supervised image classification methods. The *Maximum Likelihood* method is an example of traditional supervised image classification that involves fitting one multivariate Gaussian to the training samples for each image class in order to derive test sample class-conditional likelihoods. In recent years, a number of different machine learning algorithms have also been utilized to identify orchard trees on an individual basis. *Decision Trees* (DTs), *Random Forest* (RFs), and *Support Vector Machines* (SVMs) are the frequently preferred machine learning approaches tested for this purpose. DTs are a method of non-parametric classification that recursively divides a data set by employing tests at each branch (or node).

A root node, as well as splits and terminal nodes, may be found on this tree (leaves). Each node on the decision tree has at least two descendants and always one parent ([Friedl and Bodely, 1997](#)). Separate decision tree (DT) classifier ensembles (or RFs) have emerged as a powerful novel tool. Several trees are constructed by randomly picking the training samples and/or splitting functions of the distinct trees and averaging them to increase the robustness of the predictions. The minimum number of observations per tree leaf, the number of factors used to calculate the split at node, and the total number of trees to grow are all necessary parameters of the RF approach. Another popular machine learning technique is SVMs that minimize structural risk by learning a hyperplane strategy which maximizes the margin between input classes. Support vectors fully define the classifier and hyper-plane. A kernel function for non-linear decision boundaries implicitly maps training samples to a higher-dimensional space. Kernel function width and regularization strength affect SVM behavior ([Ozdarici-Ok, Ok, and Schindler, 2015](#)).

SOM, an unsupervised *self-organizing neural network*, is a different type of machine learning approach, however it is less popular. A two-dimensional rigid lattice holds SOM neurons. An unsupervised iterative learning algorithm based on the best matching unit adapts each neuron's weight vector to match the feature vectors ([Reis and Tasdemir, 2011](#)). *Convolutional Neural Networks* (CNNs), deep learning models originally designed for grid-patterned data such as images, learn the

spatial hierarchy of features from low- to high-level patterns automatically and adaptively. Convolution, pooling, and fully connected layers are present in CNNs. The initial two layers, convolution and pooling, extract features, and the final layer, a fully connected layer, maps them to classification output. CNN employs a large number of mathematical operations, including convolution, a specialized linear operation (Web 1). Besides CNN, other deep learning architectures (such R-CNN and YOLO) devoted for object detection have also been developed and are recently utilized for tree identification in orchards. Nevertheless, because of the complexity of tree structures, accurate delineation and the extraction of tree-related parameters remain challenging despite the advance of numerous techniques, and such topics have emerged as a prominent study area in the remote sensing and computer vision fields. A recent review article investigated individual tree detection and crown delineation using CNN ([Zhao et al., 2023](#)). The findings revealed that CNN models outperformed other methods. Data efficiency, model selection, and training strategies, on the other hand, defined its performance.

In the literature, a review article for region-based classification using remote sensing and geospatial techniques was published on the management of fruit trees and nut crops ([Panda et al., 2010](#)). That study investigated various geospatial technologies (GPS, GIS spatial modeling, advanced image processing techniques, methods of suitability map generation, orchard delineation, and validation) in addition to different remote sensing platforms (satellite, LiDAR, aerial, and field mapping) evaluated on blueberry, citrus, peach, apple, and some other species. Our motivation for preparing this review article is made clear by the fact that no previous study has attempted such a comprehensive evaluation of individual fruit trees from a remote sensing perspective to the best of our knowledge. In order to emphasize the research studies already performed and draw attention to the potential gaps in this topic, this work performs an exhaustive review of the studies conducted up to today on orchard trees. In order to accomplish this, various methods of tree extraction are studied, with particular emphasis placed on classifying fruit trees according to their corresponding climate-of-origin (tropical, subtropical, temperate). For this purpose, 22 academic journals were considered (Fig. 3), and the studies dealing with a regional classification of orchards were purposefully omitted from this review to better focus on the topic of identification of individual trees in orchards.

The structure of this article is as follows: In Section 3, we discussed the methods for digital image processing used for fruit tree extraction based on the climate of origin of the trees in the orchard. Section 4 discusses the evaluation strategies for the proposed methodologies and

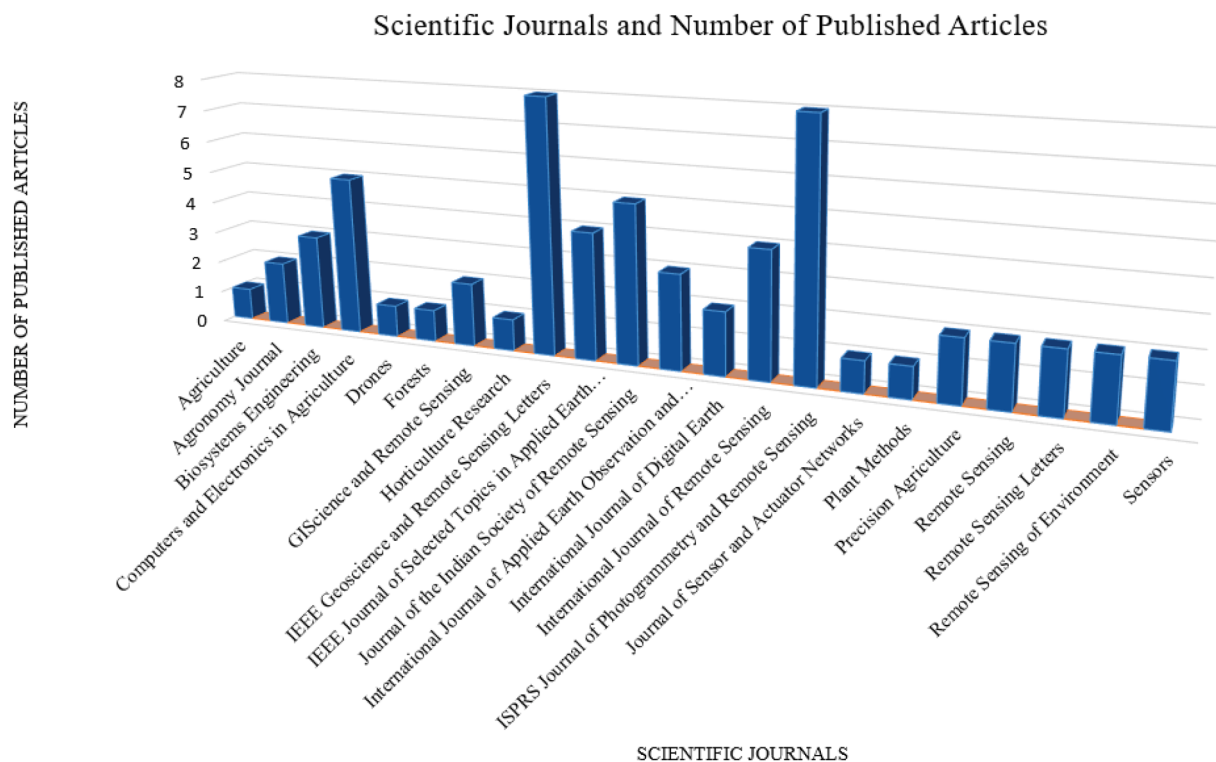


Fig. 3. Articles about individual tree detection in orchards published.

the attained accuracy. The methods and prospects of fruit tree recognition are discussed in Section 5. Section 6 concludes the document with some final thoughts.

2. Individual tree species in orchards

Fruits are primarily classified into tropical, subtropical, and temperate tree families based on their geographic origins (Fig. 4). Based on this classification, tropical fruits are fruits that grow in locations where warm climate predominates and there is no freezing temperature. *Mango* and *avocado* are the most prevalent tropical fruits found in such places. Subtropical fruits are grown in warm or mild climates, such as the subtropics and the Mediterranean, where they may withstand light frosts. In this study, *olive*, *citrus*, *hazelnut*, and *lychee* are evaluated as fruits in this category. The cultivation of temperate fruits requires cold winter climates and low temperatures. In chilly winter, fruit trees suppress their visible growth to endure the freezing period and remain robust after the season (Mohapatra et al., 2013). In this study, fruit trees

such as *apple*, *peach*, *plum*, *chestnut*, and *almond* are evaluated. Based on the data and methodology employed, this study reviewed 74 journal articles on 11 distinct orchard trees (Fig. 5). The articles examined were summarized in Table 1.

2.1. Fruit trees in tropical climates

In this section, the research that has been done on the tropical fruit trees, *mango* and *avocado*, has been organized and discussed in depth.

A method was developed to generate mango yield maps at the orchard scale using UAV-based images in West Senegal (Sarron et al., 2018). A ground sample distance of 1.30 cm/pixel was used to analyze VHR UAV photos from 15 orchard sites. Land cover maps were created by employing the GEOBIA approach to individually outline treetops and classify the land cover following the automatic generation of orthomosaics and CHM. Images were classified using the RF method. For a total of 15 orchard locations, the mean accuracy was calculated to be 89%. Also, a model was developed for estimating the yield of each individual

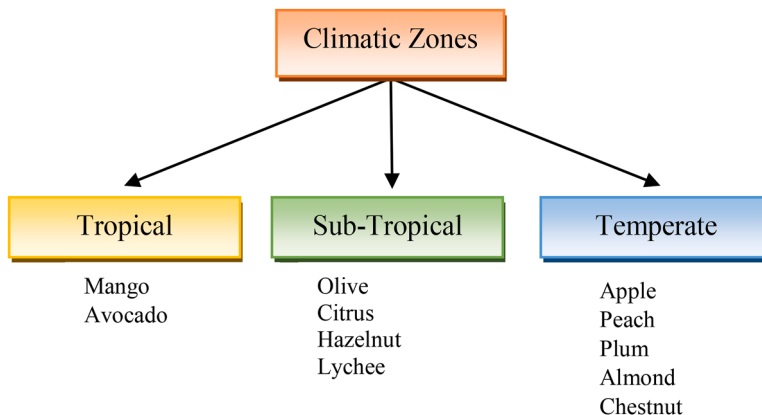


Fig. 4. Climatic zones and the types of orchard trees classified under each zone.

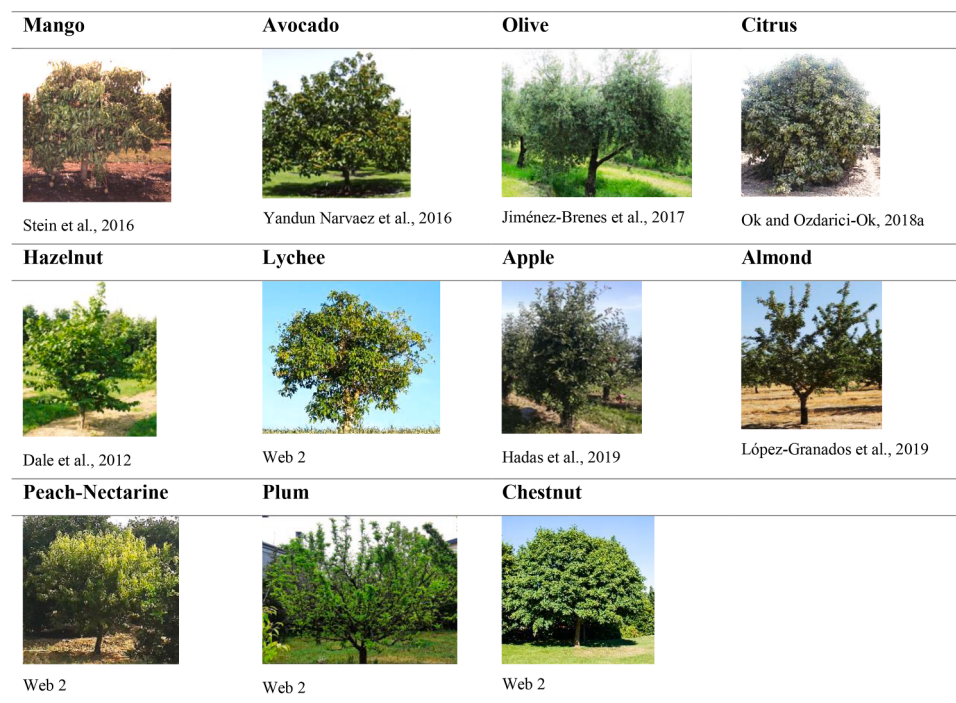


Fig. 5. The types of orchard fruit trees utilized in different journal contributions.

tree, and the resulting estimates for mango yields were favorable, with an average of around 90%. In a different study, a hidden semi-Markov model was utilized with LiDAR data collected near Bundaberg, Queensland, Australia, to segment individual mango trees (Stein et al., 2016). The primary focus of the article is on using the segmented individual trees to identify and locate mango fruits. Using multi-view geometry and a frame-by-frame method for tracking fruit, an approximate harvest estimate was achieved. Mango tree detection was accomplished using the faster R-CNN method, and the error rate was reported to be 1.36% when comparing individual trees.

Only a few research studies were devoted to the extraction of avocado trees from remotely sensed images (either individually or in groups). In a semi-automated framework, Tu et al. (2020) extracted UAV-image-derived products (CHMs, NIR, and NDVI) to mitigate the delineation task of individual avocado trees over the test site in Queensland, Australia. They also focused on multiple scenarios for UAV flight planning to extract the height of avocado trees and the related plant cover. Gomes et al. (2018) evaluated individual avocado trees through the MPP and a geometrical-optical model. They applied their approach to panchromatic WorldView-2 images comprising avocado orchards from Morro Bay in California, USA. They reported up to 95% and \approx 63% accuracy for counting and delineating avocado trees in orchards, respectively. In another study, a ground-based remote sensing system was used to collect both thermal and 3D physical parameters of avocado trees. In that study, an automatic approach was also implemented to the integration of LiDAR and thermal images to detect 3D characteristics of avocado trees in orchards using the Iterative Closest Point (ICP) algorithm (Yandún Narváez et al., 2016).

2.2. Fruit trees in sub-tropical climates

Research studies on three distinct fruit varieties, namely *olive*, *citrus*, and *hazelnut*, are organized and discussed in this section.

A deep learning model called U2-Net was used to detect individual olive tree crowns in UAV images in China (Ye et al., 2022). The proposed deep learning model called U2-Net was tested and compared to other deep learning models (e.g., U-Net, HR-Net, etc.), and the proposed model was found to be superior to the other deep learning models with

an F1-score of 95.95%. Using high-resolution single and multi-temporal satellite imagery (i.e., Planet), a deep learning model (CNN) was built to recognize olive tree fields in Morocco (Lin et al., 2021). Results were examined using widely preferred measures (precision, recall, F1-score, and overall accuracy), and each test site's overall accuracy was found to be greater than 90%. One other UAV-based tree identification study refers to the early detection of fungus problems in olive trees as part of a project (Blekos et al., 2021). In this project, the CNN algorithm was used to recognize olive trees, and model accuracy above 80% was reported. Jurado et al. (2020) developed an automated method that included multitemporal monitoring and multispectral mapping on 3D models to identify individual olive trees using a UAV-based multispectral sensor in Spain. First, a multispectral image mapping to a high-resolution point cloud was performed. Thereafter, two flight acquisitions were subjected to morphological and spectral multi-temporal analysis. Following a segmentation stage, several vegetation indices for the areas were computed. A voxel-based decomposition was investigated to estimate the height and volume characteristics of the trees. Visual and statistical analysis revealed that olive trees showed a positive trend. In a different study based on the OBIA method, UAV images were used to look at olive tree characteristics and a yield prediction model in Greece, where olive farming is reported to be important (Stateras and Kalivas, 2020). The R^2 value of the multiple linear regression model for the sloped area was calculated to be 0.6 based on the observations of 40 olive trees. Researchers also studied pruning's effects on olive tree architecture and annual canopy growth in Spain (Jiménez-Brenes, 2017). Datasets obtained before, after, and a year after pruning were used to study conventional, adapted, and mechanically pruned olive trees. 3D models and OBIA were used to analyze the geometric attributes of olive trees (canopy areas, heights, and crown volume). Ortho-mosaic and DSM were generated, and the trees were classified. Finally, each tree's geometric features were calculated. Most leaves were lost during adaptive pruning. Vegetative growth was stimulated by traditional pruning, while mechanical pruning kept it at a steady rate. In another study, checkerboard segmentation, pre-classification of trees and barren soil, tree delineation, and geometric tree measuring were applied to the DSMs (Torres-Sánchez et al., 2018b). Experimental findings showed that 95% forward overlap at 100 m altitude produced the best outcomes.

Table 1

The articles were analyzed and categorized based on the fruit types (data utilized, methods employed, accuracy information provided).

| Fruit(s) Type | Dataset(s) Utilized | Method(s) Proposed | Accuracy Information Provided | Reference |
|---------------|---|--|---|--|
| Mango | UAV (1.30 cm) | CHM & RF algorithm | ~90% (mean categorizing accuracy) | Sarron et al., 2018 |
| | LiDAR | Hidden semi-Markov Model & R-CNN | 1.36% error rate | Stein et al., 2016 |
| Avocado | UAV | CHM+NDVI | | Tu et al., 2020 |
| | Satellite (Worldview-2) | Marked Point Processes (MPP) & geometrical optical model | 95% counting, ~63% delineating accuracy | Gomes et al., 2018 |
| Olive | LiDAR, Thermal images | Iterative Closest Point (ICP) algorithm | – | Yandún Narváez et al., 2016 |
| | UAV | Vegetation classification & image segmentation & probabilistic approach & Delaunay triangulation | 77.5% recall and 70.9% precision accuracy | Illana Rico et al., 2022 |
| | UAV | Deep Learning (CNN) | >80% model accuracy | Blekos et al., 2021 |
| | Satellite image (3 m) | Deep Learning | > 90% overall accuracy | Lin et al., 2021 |
| Pear | UAV | OBIA | $R^2 = 0.6$ | Stateras and Kalivas, 2020 |
| | UAV | Vegetation indices, image segmentation & morphological feature extraction & multi-temporal analysis | Mean error height = 5 cm, Mean error in volume = $0.4m^3$ | Jurado et al., 2020 |
| | Worldview-3 (0.31 m) | OBIA & Vegetation Indices | > 90% F1 score | Solano et al., 2019 |
| | Airborne Laser Scanning | Alpha shape & PCA algorithms | 19% average error for tree height, 53% for crown base height, and 13% and 9% for the length of the longer and perpendicular diameters | Hadas et al., 2017 |
| | UAV | 3D models & vegetation indices | Voxel-based decomposition | Jimenes-Brenes, 2017 |
| | Airborne hyperspectral (50 cm) and Thermal data (62 cm) | Linear discriminant analysis (LDA) & support vector machine (SVM) | 59.0% overall accuracy of LDA, 79.2% overall accuracy of SVM | Calderón et al., 2015 |
| | LiDAR | Stepwise regression | $R^2 = 0.70$ (volume) $R^2 = 0.67$ (height) | Estornell et al., 2014 |
| | Geoeye-1 (Pan&MS) | Asymmetrical smoothing & local minimum filtering & masking & spatial aggregation & NDVI | 95% delineation accuracy | Santoro et al., 2013 |
| | CASI, QuickBird | LMRDA | $R^2 = 0.76$ and RMSE = $5.6m^2$ (CASI) $R^2 = 0.65$ and RMSE = $6.2 m^2$ (QuickBird) | Gomez et al., 2011 |
| | UAV | Deep Learning (YOLOv5) | up to 90% F-score | Tian et al., 2022 |
| Citrus | UAV | Deep Learning approach with a hybrid attention mechanism module & a feature-fusion module & a Ghost module | 90% and 81% detection F-scores | Yuan et al., 2022 |
| | UAV | Connected Component Labeling (CCL) algorithm | > 95% precision accuracy | Donmez et al., 2021 |
| | UAV | Deep Learning (CNN) | > 95% F-score | Oscio et al., 2021 |
| | UAV | Deep Learning (CNN) | 95% F-score | Oscio et al., 2020 |
| | UAV | Otsu threshold & GLCM & SVM | Segmentation accuracy = 85.27% | Chen et al., 2019 |
| | UAV | Sequential binary thresholding & Canny edge detector & Circular Hough Transform | > 80% delineation accuracies | Koc-San et al., 2018 |
| | UAV | New form of orientation-based radial symmetry transform & active contours algorithm | > 90% F-scores | Ok and Ozdarici-Ok, 2018a |
| | Pleiades-1 stereo/tri-stereo images | Correlation-based and least squares method & semi-global method | not satisfactory results | Ok et al., 2018 |
| | UAV | Orientation symmetry & local maxima with a probabilistic approach | > 90% F-scores | Ok and Ozdarici-Ok, 2018b |
| | UAV | Simple Linear Iterative Clustering (SLIC) & Deep Learning (CNN) | Overall accuracy = 96.24% | Csillik et al., 2018 |
| Hazelnut | LiDAR | Decision tree classification | > 90% overall accuracy | Fieber et al., 2013 |
| | Aerial photos | K-means image classification & NDVI+ image filtering & Hough Transform | $R^2 = 0.96$ | Recio et al., 2013 |
| | UAV | Canopy assimilation method and defining the canopy's shape | $R^2 = 0.841$ (treeheight), $R^2 = 0.765$ (radius), $R^2 = 0.508$ (canopyheight), $R^2 = -0.117$ (trunk) | Vinci et al., 2023 |
| | Ikonos (PAN:1 m), QuickBird (PAN: 0.6 m) | A new unsupervised algorithm | 0.85 and 0.61 F-scores for the sites | Aksoy et al., 2012 |
| Lychee | QuickBird MS | SOM, MLC, unsupervised object-based method | 95% overall accuracy | Reis and Tasdemir, 2011 |
| | UAV | OBIA | RMSEs around 0.60 (tree crown width); 0.25 (height) and 3.85 (perimeter) for 30,50, and 70 m flying height | Johansen et al., 2018 |
| | | | > 90% F-score | |
| Apple | UAV | Deep Learning (R-CNN) | | |
| | UAV | Structure-from-motion (SfM) | | |
| | LiDAR | Alpha-shape algorithm & thresholding & PCA & local minima | $R^2 =$ ranging from 0.81 to 0.91 99% detection accuracy | Wu et al., 2020 Hobart et al., 2020 Hadas et al., 2019 |
| | Terrestrial LiDAR | Proximal photogrammetric techniques | – | Murray et al., 2020 |
| | Aerial images | Marker Controlled Watershed Segmentation (MCWS) | 87%–97% detection accuracy, 75%–98% delineation accuracy | Niccolai et al., 2010 |
| Kiwi | LiDAR | Morphological operator & region growing segmentation | 99.4% and 61.2% precision accuracy for two test sites | Jang et al., 2008 |

(continued on next page)

Table 1 (continued)

| Fruit(s) Type | Dataset(s) Utilized | Method(s) Proposed | Accuracy Information Provided | Reference |
|----------------|-------------------------------------|--|---|----------------------------------|
| Almond | UAV | Geostatistical analysis | Coefficient of variations: 4%–14% (LiDAR), 25% (Vegetation indices) | Martínez-Casasnovas et al., 2022 |
| | LiDAR | | $R^2 = 0.94$ for three heights and 0.9 crown delineation accuracy | López-Granados et al., 2019 |
| | UAV | OBIA | $R^2 = 0.71$ | Zhang et al., 2019 |
| | Aerial image | SVM & vegetation indices | > Over 0.90 delineation accuracy | Torres-Sánchez et al., 2018a |
| | UAV | OBIA | | Camino et al., 2018 |
| | Hyperspectral and thermal imagery | Watershed algorithm | $R^2 = 0.78$ in pure vegetation pixels vs. $R^2 = 0.52$ with the warmer pixels | |
| | Mobile Terrestrial Scanning System | LiDAR volume estimation | – | Underwood et al., 2016 |
| | UAV | Conditional generative adversarial networks (cGANs) & k-means & an ellipsoid volume method (EVM) | F-measure = 0.846 | Hu et al., 2022 |
| | UAV | Adaptive threshold & morphological operation & watershed transform | > 85% R^2 values | Mu et al., 2018 |
| | LiDAR | K-means clustering & image filtering & Watershed transform | around 0.78 correlation coefficients | Pforte et al., 2012 |
| Plum | UAV | Image filtering (CHM, NDVI) & Unsupervised and supervised image segmentation | 0.53 - 0.83 R^2 | Di Gennaro et al., 2020 |
| | UAV | Segmentation & cluster isolation & feature extraction | > 97% detection accuracy, RMSE = 0.33 m (tree height) and RMSE = 0.44 m (crown diameter) | Marques et al., 2019 |
| Multiple Trees | UAV | Revised Local Transect Method | $R^2 > 0.75$ and RMSE < 14.65% | Hu et al., 2023 |
| | UAV | Deep Learning (YOLOv4) | 94% F-score | Zhu et al., 2022 |
| | UAV | Morphological image analysis & Otsu's method & image segmentation | 94% classification accuracy, 98% detection accuracy | Ponce et al., 2022 |
| | UAV | Marker-controlled segmentation algorithm | F-scores 0.88–0.99 (taxus) F-scores 0.55–0.61(olive) | Ottoy et al., 2022 |
| | WorldView-2 (Pan&MS) | Gaussian blob model & an improved tree crown model | TP = 90.09% (walnut), 82.35% (oil palm), 94.82% (vitellaria) | Mahour et al., 2020 |
| | UAV | Local maxima filtering & Watershed segmentation | > 95% accuracy | Dong et al., 2020 |
| | UAV | Cumulative Summation of Extended Maxima transform (SEMAX) | F-score = 88.8% ± 7.1% | García-Murillo et al., 2020 |
| | UAV | Deep Learning | around 76% detection rate | Pleșoianu et al., 2020 |
| | AVIRIS, EO-1 | Spectral Angle Mapping (SAM) and SVM | 78–81% overall accuracies | Kozhoridze et al., 2018 |
| | UAV | Extreme Learning Machine (ELM) method & Watershed segmentation & K-means clustering | 85.99%–98.67% overall delineation accuracy (ELM). 65%–95.99% overall detection accuracy (ELM) | Kestur et al., 2018 |
| Chestnut | WorldView-3 (Pan&MS) | A Template Matching-Based Approach | F1 score = 0.918 | Vahidi et al., 2018 |
| | Satellite image (PAN) | An edge-based probabilistic voting (Canny, Watershed algorithm, Otsu's threshold) | Low accuracies were obtained except for one site | Özcan et al., 2017 |
| | LiDAR, aerial photos, field mapping | Review article | – | Panda et al., 2010 |

Dendrometric parameters of over 1100 olive trees were analyzed using alpha-shape and principal component analysis techniques using airborne laser scanning data with an average scanning density of 4 points per m^2 collected near the city of Valencia in Spain (Hadas et al., 2017). A DTM was generated (1×1 m) with an RMSE of 0.13 m. The alpha-shape algorithm based on Delaunay triangulation was used to delineate individual tree crowns. Comparisons with the other semi-automated methods demonstrated that promising results with equal or even higher scores were obtained with the proposed approach.

A semi-automated approach was developed for olive orchards based on GEOBIA and several vegetation indices (NDVI, Modified Soil Adjusted Vegetation Index 2 (MSAVI 2), Normalized Difference Red Edge Vegetation Index (NDRE), Modified Chlorophyll Absorption Ratio Index Improved (MCARI2), derived from WorldView-3 imagery (2016) acquired on two different test sites in Italy (Solano et al., 2019). First, a merging operation was conducted to obtain a high-resolution multispectral image with 0.31 m spatial resolution. After performing multiple corrections (e.g., atmospheric, geometric), PCA was applied to the fused images to reduce correlation between spectral channels. Next, the accuracy of the identified individual tree crowns was assessed. Overall F1 scores of over 90% were reported for each test site. The biophysical properties of olive trees were studied using CASI-Airborne (seven spectral bands with 1 m spatial resolution) and QuickBird satellite images (2.5 m and 0.60 m spatial resolution) (Gomez et al., 2011). A plant

canopy analyzer was utilized to measure olive trees' crown transmittance. Individual olive crowns were detected and delineated using an algorithm (i.e., LMRDA). CASI hyperspectral images exhibited the best accuracy, with an R^2 and RMSE of 0.76 and 5.6 m^2 , respectively. QuickBird panchromatic images provided relatively poor results with an R^2 of 0.65 and 6.2 m^2 . It was also indicated that CASI vegetation indices better estimate tree crown transmittance. In a different study, LiDAR data (November 2009) with low pulse density points over 29 circular plots (20 m radius) in Spain was used to assess olive tree height and volume (Estornell et al., 2014). Volume and height were estimated using stepwise regression, and R^2 values were reported to be 0.70 and 0.67, respectively.

Citrus trees were extracted from UAV imagery in a recent study using the YOLOv5 method. To efficiently identify the citrus trees and extract related coordinates from the orchard orthophoto image, the YOLOv5 model was used to train the remote sensing dataset. F1-scores of up to 90% were obtained for two test sites (Tian et al., 2022). Connected Components Labeling (CCL) algorithm is followed by a series of morphological operations applied to high-resolution UAV images. Results were reported for two agricultural patches with accuracy and precision both greater than 95% (Donmez et al., 2021). A deep learning technique based on CNN was presented to identify plantation rows and count citrus plants (Osco et al., 2021). Promising results were reported over a 95% F1-score when results were compared with other deep

learning methods (HRNet, Faster R-CNN, and RetinaNet). A different study was conducted to estimate the number of trees with a CNN method using UAV multispectral images (green, red, red-edge, and near-infrared) in dense Brazilian citrus orchards covering approximately 70 ha (Osco et al., 2020). In the analysis, a 2D confidence map estimation approach was used to recognize individual trees. Green, red, and near-infrared bands provided better performance with a 95% F1-score when related parameters were adapted. Besides, results were compared with the other state-of-the-art object-based methods, i.e., Faster R-CNN and RetinaNet. Using UAV imagery, the effects of different color spaces on the segmentation of citrus trees were investigated (Chen et al., 2019). The proposed method consisted of three fundamental steps. The first step was image pre-processing using the correct color space. The second step was about the selection of the region of interest, and the third step was about segmenting the tree. SVM was employed during the segmentation phase. The results revealed that segmentation accuracy reached $85.27\% \pm 9.43\%$. A different study based on the circular Hough transform applied to UAV images and DSMs was performed on three test sites selected in the Mediterranean region of Antalya, Türkiye (Koc-San et al., 2018). Methodological steps include the application of sequential binary thresholding, Canny edge detection, and the circular Hough transform, followed by a series of pre-processing steps (including data calibration, image matching, and filtering). Over 80% delineation accuracy was obtained for each test site.

2D delineation of citrus trees from VHR UAV-based dense photogrammetric surface models on eight test sites, including varying citrus orchards having different densities and canopy sizes, was proposed by Ok and Ozdarici-Ok (2018a). The approach proposed a new form of orientation-based radial symmetry transform directly applied to DSM to detect tree candidates. An automated active contour was developed to delineate individual citrus trees, followed by interest and influence region strategies. Erroneously detected regions were eliminated with two effective strategies. Results over 90% were observed for all test sites when the overall pixel- and object-based F1-scores were evaluated. An accuracy assessment study was carried out on Pleiades-1 stereo and tri-stereo DSMs in citrus orchards in Mersin province, Turkey (Ok et al., 2018). Three different image matching methods—local methods (correlation-based and least squares methods), semi-global methods (semi-global matching (SGM)), and global methods (SIFT-flow)—were tested on three test sites. Experimental results indicated that the SGM forward-backward stereo combination provided the best results for two test sites, while none of the methods could meet expectations because of the relatively coarse GSD (0.7 m) of the Pleiades-1 sensor. In a different study using DSM as input, Ok and Ozdarici-Ok (2018b) proposed a new approach to the automatic detection of citrus trees by combining orientation symmetry and local maxima (LM) cues with a probabilistic approach. Results revealed that F1-scores over 90% were achieved with eight different test DSMs, and the results were compared with the state-of-the-art methods.

Citrus trees were identified using UAV imagery and the CNN method in a different study (Csillik et al., 2018). An overall accuracy of 96.24% was calculated using the CNN method. However, the study's flaw was the presence of multiple crowns in a single, massive tree crown. GeoEye-1 panchromatic and multispectral images of a southern Italian citrus orchard were used to automatically identify citrus trees (Santoro et al., 2013). Asymmetrical smoothing, local minimum filtering, masking, and a spatial aggregation operator were applied to 6500 tree images of various ages and plantings. A 1.5 m-radius 7×7 circular window was chosen, and local standard deviation and NDVI were used as masks. As a result, 95% accuracy was reported.

Full-waveform LiDAR data were analyzed for the classification of Australian citrus orchards (Fieber et al., 2013). The decision tree classification was used to classify three different classes (citrus trees, grass, and ground) and relied on just a pulse with a backscattering coefficient without neighborhood relationships or object-based knowledge. Single-peak waveforms and multiple returns were utilized to

differentiate the classes from each other. The overall accuracy was computed at over 90% when aerial images and elevation data were used. Recio et al. (2013) presented an application of Hough transform to recognize citrus orchard planting patterns. From three-band (green, red, and near-infrared) aerial images collected in the Valencia region of Spain, a plot-based automated approach was developed to obtain individual trees and their attributes for 300 citrus orchards. To identify tree classes, an unsupervised K-means classification technique was tested, followed by an image filtering step. Following the automatic extraction of tree and soil data from the NDVI image, a Laplacian filter was applied to the NDVI image to obtain sharper edges for tree crowns. The Hough transform was then applied, and an R^2 value of 0.96 was reported.

Since hazelnut trees typically take the form of bushes, it is very difficult to separate them individually (Dale et al., 2012). As a result, no published research on the identification of individual hazelnut trees exists, and there is limited research on the classification of these trees. One recent study was conducted using 3D point clouds generated from UAV images to calculate hazelnut canopy size and volume, and the results were compared to traditional manual methods (Vinci et al., 2023). Two methods were used to calculate the volume of the trees: canopy assimilation into a cylinder and clearly defining the canopy's shape. The results showed that the radius, canopy height, and tree height had high correlation coefficients, while the correlation coefficient for the trunk was extremely low. A self-organizing map (SOM) was used to classify hazelnut orchards in Trabzon, Türkiye (Taşdemir, 2012). The article's novelty was learning vector quantization in SOM instead of centroid-based hierarchical clustering. QuickBird multispectral images covering 5 km^2 were used to classify hazelnut, forest, urban, bare area, and farmland. Traditional SOM, Maximum Likelihood Classification (MLC), and unsupervised object-based methods were also examined. The proposed method offered the maximum overall accuracy of over 80%, despite hazelnut and other forest types' strong spectral similarity. An unsupervised algorithm was proposed to automatically detect and segment hazelnut orchards using VHR IKONOS and QuickBird images (Aksoy et al., 2012). Two different datasets (panchromatic) IKONOS (1 m spatial resolution taken in 2007) and QuickBird (0.6 m spatial resolution taken in 2008) with 15 subscenes and 7 subscenes of Google Earth images acquired from the Black Sea and Aegean coasts of Turkey, respectively, were utilized. First, multi-granularity isotropic filters were used to enhance potential tree locations. Second, the planting regularity of the hazelnut orchards was measured with projection profiles, in which oriented sliding filters were used to examine multiple orientations. Then, the computed regularity scores were used to segment the analogous planting patterns and extract the tree crown boundaries. In the orchard detection case, the proposed algorithm provided a performance of around 85% F1-score, although marginal F1-score of 61.42% were also observed. Reis and Taşdemir (2011) proposed a classification system using spectral and spatial information for hazelnuts and other areas in the Black Sea region using pansharpened images (4 spectral channels). Their method computed panchromatic Gabor features at four scales and six orientations. Gabor characteristics were preferred because of their resemblance to human frequency and orientation representations and good localization abilities. Four classes (hazel orchard, woodlands, agricultural areas, and non-vegetation) were defined during supervised (MLC) and unsupervised (SOM) image classification methods with calculated Gabor features. Although it's an unsupervised method, the SOM algorithm with multi-temporal spectral information and Gabor features had the highest classification performance (95% overall accuracy and 0.93 Kappa value). The MLC algorithm had similar results to SOM (92% overall accuracy and 0.88 Kappa value).

There are hardly any studies of the delineation of the lychee tree in the literature. An OBIA method with different flying heights (30, 50, and 70 m) was used to perform multispectral UAV imaging to extract the structural properties of lychee trees before and after pruning. The results were evaluated for various flying heights, and it was discovered that pruning and flying heights may influence tree structural properties

(Johansen et al., 2018).

2.3. Fruit trees in temperate climates

This section organizes and discusses research studies on five different fruit tree varieties: *apple*, *almond*, *peach-nectarine*, *plum*, and *chestnut*.

One recent example of detecting apple trees was a deep learning method (U-net) to examine tree crown data (Wu et al., 2020). The method consists of using the faster R-CNN and a pruning strategy to detect, count, and segment apple trees. UAV images were used to test a total of 50 fields, and promising results were obtained with an F1-score of more than 90%. Hobart et al. (2020) measured the growth height of apple trees using UAV photogrammetry using structure-from-motion (SfM). LiDAR data was used for validation, and R^2 values ranging from 0.81 to 0.91 were calculated. The study emphasized the significance of UAV imagery with a high forward overlap ratio. In another study, Gaofen-1 satellite images were used to test image classification approaches such as the integrated unsupervised-supervised classification method, SVM, nearest-neighbor, and decision-tree methods for the recognition of apple trees in orchards in China (Liu et al., 2021). The unsupervised-supervised classification approach used on a four-band multispectral image with a resolution of 16 m involves the MLC method followed by ISODATA classification. Results of over 90% were observed for each image classification strategy. A framework was developed to investigate the integration of automatic template matching with marker-controlled watershed segmentation (MCWS) for the recognition of individual apple tree crowns (Niccolai et al., 2010). High-quality optical images with varied resolutions (spatial, spectral, and temporal) were used to recognize treetops by manual digitization and template/correlation selection. The results showed that the location of the initial markers had a significant impact on the final segmentation result.

A method was developed to examine the geometry parameters of apple orchards using a LiDAR-equipped UAV (Hadas et al., 2019). The alpha-shape method was used to distinguish tree crowns, followed by a simple threshold to minimize low vegetation reflections. PCA was applied, and local minima were then used to distinguish crown rows. In that study, 649 of 655 trees (99%) were correctly identified. The calculated correlation coefficient for tree height was 0.96, while for crown base height it was reported to be 0.70. Another methodology was presented to identify the geometrical characteristics of apple trees with photogrammetry and terrestrial LiDAR data in a test site in southeast England (Murray et al., 2020). A total of 140 trees with approximately 5–8 years of age were examined during leaf-off conditions in the winter season of 2017–2018. Results revealed that correlation analysis performed with LiDAR data provided superior outputs to the photogrammetric method. Airborne LiDAR data was used to evaluate apple orchards in Canada (Jang et al., 2008). Two orchards with apple trees ranging from 0.8 m to 6 m in height were studied. The airplane was equipped with LiDAR and a multispectral camera (blue, green, red, and near infrared) to obtain point clouds and vegetation spectral signatures, respectively. Inverse Distance Weighting (IDW) interpolation was utilized to transform LiDAR data to pixel values and generate raster images of vegetation and ground. The tree crown delineation model had several steps, including smoothing LiDAR data to remove noise, masking, and applying local maxima and local minima filters to locate tree top locations and crown borders. Multiple post-processing processes were also performed, and the final step was region-growing segmentation. The results showed that the accuracy of LiDAR tree detection was 99.4% at the first test site but dropped to 61.2% at the second.

Management zones in hedgerow almond orchards were identified using canopy parameters derived from LiDAR and vegetation indices from UAV images (Martínez-Casanovas et al., 2022). Geostatistical analysis was carried out to interpolate continuous representations of the variables. The geometrical and structural parameters derived from NDVI produced the best results. The prediction of almond yield models at

orchard level (early and mid-season) was performed by a machine learning approach in California, USA (Zhang et al., 2019). Three different variables were included in the analyses: grower data (planting year, historical yield, cultivar variety, and composition); weather data (monthly mean daily max and min temperature, monthly accumulative precipitation, and hourly temperature); and remotely sensed data (NAIP RGB imagery with 0.6 m and Landsat MS imagery). Using the aerial imagery, the canopy cover percentage was first produced with SVM. Next, vegetation indices of NDVI and enhanced vegetation index (EVI) were derived from Landsat images. After testing different machine learning approaches (linear regression, support vector regression, neural networks, RF, and stochastic gradient boosting (SGB)), SGB was applied to predict the early- and mid-season yield of almond trees. Accuracy values of R^2 of 0.71 were observed with the machine learning model. 3D physical characteristics and flowering traits were examined with an UAV-based platform on two almond orchards southern Spain (Lopez-Granados et al., 2019). First, 3D point clouds were generated by UAV images taken with 93% and 60% forward and side overlaps, respectively, at 50 m flight altitude and 15.3 mm GSD. Next, the OBIA algorithm, including DTM generation, tree crown delineation, point cloud slicing, and describing 3D features of almond trees, was used to estimate the geometric characteristics (such as tree height, crown projected area, and crown volume) of each individual tree. Validation of the results revealed a consistency between the estimated and reference tree heights (R^2 of 0.94) and the result of crown delineation accuracy (0.9 in a range from 0 to 1). An automatic OBIA technique combined with photogrammetric point clouds derived from UAV was conducted to map 3D geometric features (height, area, and volume) of almond trees in Spain (Torres-Sánchez et al., 2018b). Two different plantation years (March 2016 and September 2017) were selected based on phenological phases (leaf-off and leaf-on) of almond trees to map crown volumes and monitor the development of leaf conditions. True color images acquired with a 50-m flight attitude and 15.3 mm ground sampling distance were used in the analysis. The proposed OBIA methodology consists of multiple steps: DTM generation, center detection of tree crowns, removing small centers by a defined threshold, delineation of tree crowns by the segmented normalized digital surface model (nDSM) with a multi-resolution segmentation algorithm, and point cloud slicing to almond crown characterization to compute volumes. Similarities of over 90% were observed when the automatically delineated and reference tree crowns were compared.

Although water stress detection is not the direct subject of this review, an interesting article on this subject was included in this study since an object-based approach was used to find tree crowns (Camino et al., 2018). In that article, the solar-induced chlorophyll fluorescence and the crop water stress index variability within the crowns of almond trees were studied southern Spain. Fluorescence retrieval was evaluated by hyperspectral imagery with 20 cm spatial resolution from the whole tree crowns using an automatic object-based image analysis method. Thermal imagery with 25 cm resolution was also used to measure the distribution of canopy temperature using segmentation algorithms. Within crown segmentation, an automatic object-based crown detection algorithm based on watershed segmentation was used. NDVI was then used to separate sunlit vegetation from non-vegetation pixels. The outputs highlighted the importance of using high-resolution hyperspectral and thermal images. The automatic segmentation algorithm reduced the effect of the operator when defining regions of interest and minimized the bias.

Almond trees were mapped individually in a different study using terrestrial LiDAR and a vision sensor to obtain canopy volume, flowers, fruit, and yield (Underwood et al., 2016). The 3D models are used to calculate the volume of the canopy, and images are classified to determine the flower and fruit densities. A strong linear relationship (R^2 of 0.77) was found between LiDAR canopy volume and yield, as well as fruit density (R^2 of 0.71).

Deep learning approaches for peach trees from UAV-based images

were investigated in China (Hu et al., 2022). The method relied on clustering and k-means, followed by a deep learning architecture known as conditional generative adversarial networks (cGANs). In the final step, the crown volume was estimated using the ellipsoid volume method (EVM). By providing an average F1-score of 84.6%, the proposed framework outperformed other deep learning models (fully convolutional network, U-Net, and SegNet21). A different method was presented to identify individual peach tree crowns by high resolution multi-temporal images (RGB mode better than 1 cm per pixel) derived from UAV in two orchard plots (≈ 1.65 ha) in Japan (Mu et al., 2018). Two different DSMs were produced from UAV images. An adaptive threshold was used to recognize tree crowns in the analyses. Branches of the trees were merged by a morphological operation (closing), and the boundary of tree crowns was obtained. Watershed transformation was applied to the DSM to define individual tree crowns. On average, R^2 values above 85% were obtained.

There are also a limited number of studies for the recognition of plum trees, in which two automated canopy cover techniques were assessed for the recognition of 4- and 5-year-old plum trees in a test site with 180 trees in Brandenburg, Germany (Pforte et al., 2012). The first method contains a calculation of leaf coverage based on NIR image analysis. Another method is to count the number of laser scanner (LiDAR) pulses for each tree. In the image-based analysis, a clustering procedure was used to assess the visible percentage of leaf cover, with 12 clusters chosen based on statistical criteria (i.e., standard deviation, mean, median, mode, maximum, and lowest values). A watershed technique was used to segment the visual objects. A binary image was created using a morphological operator (closing) based on the results. In the LiDAR-based analysis, a suitable laser rangefinder was chosen based on many tests and put onto a tractor in a top-down view. For LiDAR and image-based analysis, the correlation coefficients of estimated leaf areas were 0.87 and 0.79, respectively.

An automated UAV-based image segmentation approach was applied to chestnut orchards (Di Gennaro et al., 2020). That study extracted geometric features of chestnut using supervised and unsupervised crown segmentation, followed by a double filtering process based on vegetation index threshold and CHM. R^2 results for supervised and unsupervised segmentation approaches ranged from 0.76 to 0.95, which might be a potential for monitoring vast areas quickly and affordably. Other UAV-based chestnut methodology was performed through image segmentation, cluster isolation, and feature extraction steps. Sentinel-2 satellite data and low-density LiDAR point clouds were used to map chestnut trees in small plantation areas (Alonso et al., 2020). The image classification algorithms RF, SVM, and XGBoost were used in the analyses. Individual trees were detected using the local maxima algorithm calculated from CHM, and their crown surfaces were delineated using two-dimensional (2D) tree shape reconstruction and LiDAR point cloud canopy segmentation. The overall detection accuracy and R^2 values were found to be 81.5%, 96%, and 0.83, respectively. One significant aspect of the study was the plantation-level analysis, which allowed for a comparison of different plantation periods using a multitemporal analysis. The suggested method provided RMSEs of 0.44 m for crown diameters and 0.33 m for tree heights (Marques et al., 2019).

3. Studies involving multiple types of fruit trees

This section discusses the studies that have been conducted on a more comprehensive range of fruit tree species at the same time.

Optimal flight and smoothing parameters for detecting taxus and olive trees were determined using UAV images in Belgium (Ottoy et al., 2022). For that purpose, the transferability of the developed marker-controlled segmentation algorithm was tested. It was discovered that the processing parameters, rather than the flight parameters, had a significant impact on the accuracy. A 3×3 pixel smoothing window performed best (F1-score of 0.99) compared to no smoothing and other sizes. An improved YOLOv4 was proposed for the reliable and fast

detection of tropical orchard trees (mandarin orange) in China's Zhejiang Province (Zhu et al., 2022). To accomplish this, 600 images of varying sizes, growth conditions, and shading levels were collected. TensorFlow was used to train the models. The results indicated an F1-score of approximately 94%. It was determined that the method is practical for detecting and counting orchard canopies. Using morphological image analysis and UAV-based aerial images, an automatic delineation methodology for tree crowns was examined (Ponce et al., 2022). In that work, aerial images were segmented and then subjected to a variety of morphological processes, yielding results with an F1-score of 94% for delineation and 98% for detection of (lemon, orange, and olive). A local transect method for detecting individual crown widths in UAV images was proposed for three different sites with different tree types, including citrus orchard trees (Hu et al., 2023). In addition to the α (adjustment parameter to reduce the influence of shadow and background), β (percentile parameter to remove outliers), smoothing effects were investigated in the study by defining different smoothing sizes in the study. When appropriate parameters and window sizes were chosen, accuracies of $R^2 > 0.75$ and $RMSE < 14.65\%$ were observed. A deep learning method based on a single shot detector (SSD) model was developed to detect and classify individual apricot, plum, and walnut tree crowns with the other coniferous trees (Pleșoianu et al., 2020). The ensemble models are put to the test at three test sites with significantly different spatial patterns using a variety of configurations of very high-resolution UAVs, aerial imagery, and elevation data. It was concluded that two participant single models improved detection performance and accuracy by 3–18%, and RGB information was the single most influential factor in identifying species.

Individual citrus and avocado trees were detected by a morphological transform called Cumulative Summation of Extended Maxima transform (SEMAX) with multiple number of processes (including cumulative summation, extended maxima, influence zones, marker image, morphological gradient, watershed) on DSMs (García-Murillo et al., 2020). The results were tested using the F1-score and computed to be $88.8\% \pm 7.1\%$ for the proposed method. For walnut, oil palm, and vitellaria trees, an automated individual tree detection method based on a Gaussian blob model was proposed (Mahour et al., 2020). Individual tree objects were detected using a two-step process with Worldview-2 imagery. The first is based on a Gaussian blob model to recognize tree crowns, and the second is related to a model improvement. When the proposed model was compared to traditional methods, an improvement of about 10–20% in true positive detections was observed at the end of the analysis. Other study was conducted to extract information about individual trees from high-spatial-resolution UAV-based images in Eastern China (Dong et al., 2020). Both apple and pear trees were analyzed in the study. Analyses start with the generation of an orthophoto mosaic, DSM, DTM, and a digital height model (DHM) from UAV images. The second step includes removing background information from the image with a height threshold derived from DHM and an Otsu threshold computed for the Excess Green minus Excess Red (ExGR) index derived from the mosaic. In the final step, individual tree crowns were detected with local maxima filtering and watershed segmentation. Results demonstrated over 95% accuracy for the test sites. In another study, a neural network-based spectral and spatial method was used to detect, delineate, and count banana, mango, and coconut trees with two UAV-based sensors on five test sites (Kestur et al., 2018). The study consists of three main stages, including a supervised classification method using the Extreme Learning Machine (ELM) algorithm to obtain tree crown and non-tree crown objects. The watershed segmentation method was used to delineate individual tree crowns. The last step includes the validation part of the study, in which the K-means clustering method was applied to the results for comparison. Better results were observed for the ELM method. Another article describes a collective sensing approach used by Citizen Science (CS) tree mapping projects to map urban orchard trees using very high resolution (VHR) optical remotely sensed data (Vahidi et al., 2018). A template matching

(TM)-based individual tree crown (ITC) detection method was developed to extract urban orchard trees from VHR optical imagery with an acceptable degree of completeness (92.7%).

Multi-date airborne (AVIRIS) with 15.5 m GSD and 224 spectral channels and space-borne (Earth Observing 1-EO-1) hyperspectral images covering 220 spectral bands with 30 m GSD acquired from different locations in California, USA, were used in the analyses (Kozhordze et al., 2018). Remote sensing indices were calculated to estimate the biochemical characteristics of trees. Spectral Angle Mapping (SAM) and Support Vector Machine (SVM) methods were conducted to classify tree species (Pistacia, almonds, and grape). Results revealed similar accuracies between SAM and SVM (difference of 1–2%). AVIRIS images provided the highest overall accuracies (77–81%). Texture-based research about automatic recognition of uprooted orchards with orthophotos (with 0.25 m spatial resolution) was presented in the northern part of Spain (Ciriza et al., 2017). Different orchard types (e.g., apricot, almond, cherry, plum, peach, apple, walnut, pear, and black-thorn) growing in different geometric patterns (regular, linear, and random) were analyzed in that respect. First, textural features were computed from orthophotos based on the second-order statistical features (homogeneity, dissimilarity, contrast, entropy, angular second moment, mean, standard deviation, and correlation) with different directions (0°, 45°, 90°, and 135°) of the gray level co-occurrence matrix (GLCM) and wavelet transform. After that, a discriminant analysis was performed based on parcel-based manner. With the help of the parcel-based classification, a linear combination of textural features was generated, and, in this way, the highest discrimination was computed between the uprooted and orchard classes. The true positive and accuracy of the features were computed at over 80% and 88%, respectively. A probabilistic voting approach was proposed to detect tree crown detection and delineation with satellite images (Özcan et al., 2017). They tested panchromatic satellite images obtained from the Google Earth platform containing 13,476 olive, peach, pear, and citrus trees. An edge-based probabilistic voting method was proposed. First, five different well-known edge-detection algorithms were tested to obtain edges from panchromatic satellite images, and the Canny approach provided the best result. Second, probabilistic votes derived from the computed edges were used for the detection of tree crowns. Next, to segment each object individually, watershed segmentation was applied. In a final step, Otsu's threshold was used to obtain interested individual trees. The proposed method provided above 80% completeness, correctness accuracies and above 70% quality values, respectively.

4. Discussion

This section provides an overview of the discussions and future prospects regarding the identification of fruit trees for each specific orchard type. The discussion covers assessments of the algorithms, types of images employed, limits of the proposed approaches, and evaluation of the accuracy indicators employed.

It has been noticed that various techniques and sensor types were applied during the analyses to identify the orchard trees. When the different sensor types were examined, it was found that the analyses used multispectral and panchromatic satellite images (GeoEye, Quick-Bird, ResourceSat LISS IV, Cartosat-1, GF-1, etc.), hyperspectral images (AVIRIS, CASI, etc.), LiDAR data, and VHR optical UAV-based multispectral images. Using the images various image-derived products (CHM, DSM, etc.) and multiple vegetation indices (NDVI, Modified Soil Adjusted Vegetation Index (MSAVI), NDRE index, Modified Chlorophyll Absorption Ratio Index Improved, etc.) were produced for orchard tree type recognition. The red-edge region of the spectrum was found to be superior for distinguishing between orchard varieties, and according to Jurado et al. (2020), NDRE yielded superior results to other vegetation indices regarding the separability of trees. However, note that strong correlations were observed between the NDVI, GNDVI, and NDRE values (Recio et al., 2013; Santoro et al., 2013, Solano et al., 2019). Several

image fusion algorithms (Brovey, Hue Saturation Value, etc.) and statistical outputs of gray level patterns were utilized in the analyses. PCA, Canny, and other edge detection algorithms (Sobel, Prewitt, Roberts, LoG, etc.), Circular Hough Transform, Watershed algorithm, and the Fast Radial Symmetry Transform were used to process the images (Dong et al., 2020; Koc-San et al., 2018; Camino et al., 2018; Ok and Ozdarici-Ok, 2018b; Özcan et al., 2017; Niccolai et al., 2010). Principal Component Analysis (PCA) was a popular method for mitigating the correlation problem of multidimensional data (Hadas et al., 2019). In addition, well-issued morphological post-processing operations (dilatation, erosion, etc.) were investigated to eliminate tree crown gaps, thinning polygon lines, and eliminating dead ends (Ponce et al., 2022; Mu et al., 2018; Jang et al., 2008). The analyses employed numerous unsupervised (K means, ISODATA, SOM, etc.) and supervised (KNN, MLC, RF, SVM, Neural Network, CNN, etc.) image classification methods. With the introduction of deep learning techniques, data augmentation techniques were also implemented to compensate for the lack of data (Pleșoianu et al., 2020). It was suggested that image platforms for fruit plant identification should be chosen based on the size of the orchards and the desired level of detail.

For the purposes of micromanagement operations involving fruit trees and nut crops, advanced remote sensing and geospatial techniques are prerequisites. With the use of surface models, surrounding crops with lower elevation values were successfully differentiated from other types of trees in the area. Therefore, this form can help to quickly get an overview of the different types of crops. The use of techniques such as robust time-series filtering and interpolation in the studies can lead to the acquisition of more trustworthy data from NDVI for the analyses. It is possible for misclassification to occur because of the heterogeneity of the uprooted parcels as well as the uniformity of the orchard parcels when there is a low contrast level between the orchard class and its ground. This can reduce the accuracy of the analysis. One other restriction on this type of research is threshold selection, which necessitates prior knowledge to define. Another flaw in the methods is the presence of multiple maxima within a single tree. More efforts are required to address these issues.

The concept of detection and delineation in orchards was numerically evaluated using a variety of assessment methods. The first step in any study that employs a numerical evaluation strategy is to create a reference (ground truth). Tree centers and crown boundaries are common examples of ground truth data. Tree detection is accomplished by identifying the locations of tree canopies, and tree crown delineation is completed by describing the outlines of tree crowns. Tree centers are digitized by hand or with the help of other image processing techniques (like local maxima), and crown boundaries are mapped by hand using true ortho-mosaics and/or DSMs with binary masks of the test sites. The final performance of the proposed approaches is measured by comparing the findings with the reference information. In both the detection and delineation stages, precision, recall, and the F1-score are typically used as measures of detection performance (Ponce et al., 2022; Ok et al., 2018). One other popular measure that computes the percentage of correctly classified pixels is overall accuracy (Dong et al., 2020). Intersection-over-union (IoU), also known as the Jaccard index, is another standard evaluation measure used in tree detection studies to compute true positive and false positive predictions (Ponce et al., 2022). Among the overall similarity measures for the detected and ground-truth objects, completeness, correctness, and OQ₀ are typical measures used in the validation of the orchard trees (Torres-Sánchez et al., 2018b). The overall quality of OQ₀ for each tree object shows what percentage of the total number of objects in the image classification result and reference data are matched (Torres-Sánchez et al., 2018a). The coefficient of determination (R^2) of the linear regression between the detected trees and the reference number of trees can also be used to assess the overall performance of the algorithms. The counting performance of the detected trees is also measured using mean absolute error (MAE), counting accuracy (ACC), and root mean squared error (RMSE) (e.g. Wu

et al., 2020). MAE and ACC represent the accuracy of the prediction, while R^2 and RMSE represent the performance of the models employed. Lower values for MAE and RMSE indicate improved counting performance (Wu et al., 2020).

Despite all these evaluation methods, tree crown delineation remains a challenge. The location of the detected objects, even if the radius is correct, is one of the most frequently encountered issues. The other is due to crown size radius differences from the actual tree crown radius, as the crown size can be larger or smaller than the actual tree crown. Another issue is the shape of the tree crowns. Even if the total area is correct, the reference tree crown (the actual one) may not be a circle or an ellipse. Consequently, instances where all these issues coexisted also arose in studies where tree crown boundaries were determined (Gomes et al., 2018). According to several studies (Ponce et al., 2022; Zu et al., 2022; Hadas et al., 2019; Ok and Ozdarici-Ok, 2018b), performance rates of 90% or higher can be attained if the fruit tree planting intervals in the test areas are both sparse and regular. However, studies show that more research is needed in areas with a variety of ages and planting combinations, especially in places where the crowns of mature trees overlap. It has also been argued that the results of some studies fall short of expectations (see, for example, Özcan et al., 2017). Additionally, using consistent flight configurations when collecting images is critical (Johansen et al., 2018) because flying at different heights may lead to varying measurements of tree structures. Analyses indicate that a forward overlap ratio of 80% is essential for the generation of dense point clouds. Below this ratio, poor results may reduce the density of generated point clouds, thereby decreasing the accuracy of tree height estimations (Tu et al., 2020). One of the limitations of the related studies is that they all use rule-based methods, which makes expanding the findings to other tree species difficult (Fieber et al., 2013). Furthermore, proper care must be taken when applying image segmentation methods, as the results of the segmentation have an immediate impact on the overall performance. As anticipated, it's possible to enhance the outcomes by employing various post-processing methods (Chen et al., 2019; Csillik et al., 2018).

The fundamental limitations of mango-based research lie in the fact that the algorithms rely on the assumption that the geometrical properties of trees. It was presumed that trees have a shape like a dome, and adequate lighting conditions were used to confirm this assumption. The other concern is the amount of tree canopy that is obscured. According to the test sites involved in previous studies, there is either no overlap at all or very little overlap between different tree crowns. When building a mask, ambiguity due to fruit bunching, ground removal errors, missing frames, and platform oscillation are all potential reasons for algorithmic failure (Stein et al., 2016). Despite encouraging results from a variety of orchard settings, there is still a substantial constraint associated with the system's reliance on threshold (Sarron et al., 2018).

According to the avocado fruit, one of the major findings is that the morphological reconstruction process with temperature data provides noticeable improvements during extraction (Yandín Narváez et al., 2016). Therefore, although numerical results related to thermal data were computed in laboratory conditions in terms of both spatial and thermal aspects, thermal information (i.e., average temperature) might play an important role even in a real environment and related conditions. According to UAV flights, quality was improved via a high solar elevation angle with UAV flights among hedgerows and low image pitch angle values.

It was found that most research on individual trees focuses on either citrus or olive trees. Some of the difficulties of citrus detection include incorrect time selection during data collection and a lack of information regarding the texture of the fruit. In research on the detection of citrus trees, the performance of image classification was shown to be highly dependent on the parameters chosen and the balancing methods utilized. Time spent processing is of critical importance. On the other hand, many of the shortcomings of the various image classification algorithms (like CNN) might be attributed to the lengthy processing times required

for training sites (Kawashita Kobayashi et al., 2019). The reliability of the maps that are created can be improved through the integration of DSM with the images (Jiménez-Brenes et al., 2017). Concerning the olive tree, which grows natively in the Mediterranean region's south, most studies on olive trees are conducted in Spain. In addition to optical and LiDAR data, inferences are drawn from DSMs generated from optical images. In this context, plant indices and OBIA methods are among the most utilized methods. When the olive tree studies were investigated, it was revealed that indices of vegetation, such as the NDVI, showed promising results in their ability to distinguish between various planting patterns. The red-edge area of the electromagnetic spectrum plays a key role in the process of identifying the vitality of plants. According to the findings of the research conducted, 3D point clouds have the potential to achieve high levels of accuracy, and LiDAR data can successfully identify important tree crown features. The authors argue that there should be a requirement for more investigations to achieve higher levels of accuracy.

Based on the findings of the analyses of hazelnut trees, it is possible to state that incorporating various rule sets into the classification process can improve the results. Additionally, the accuracy of the results can be improved through the utilization of multi-temporal images and/or an increase in the number of spectral bands. By combining spectral and spatial information in a more efficient manner, image classification systems can be enhanced. The outcomes of the analysis can be improved through post-processing techniques. UAV and satellite images are primarily used in apple tree determination studies. Studies of apple trees revealed that UAV systems equipped with LiDAR are important for the detection of the geometric characteristics of orchards. On the other hand, it is vital to ensure the reliability of the methodology to search for the consequences of the results on other tree species, flight height, and the effect of point cloud density. It is possible that the relationship between NDVI and a variety of elements, including climatic and anthropogenic, will influence the trend line. The low findings could be explained by a lack of filtering processes for ground and non-ground points, a low density of LiDAR point data, the presence of small trees, irregular tree crown shapes, holes, and overlapped branches, or by any combination of these factors. There is a possibility that the accuracy of the results will worsen due to the relatively limited test locations and sparse plants. As a result, further analyses are necessary to be performed at a variety of test sites using multiple resolutions.

Research studies of almond trees revealed that the data variable of historical yields is very important to control the temporal and spatial variation of almond trees. One main limitation is insufficient base learners, which can cause the models to fail. Considering the peach-nectarine, the proposed approaches were found to have reasonably good accuracies. The use of adaptive threshold, limitations of image segmentation, and low DSM resolution were stated as reasons for the poor outcomes.

5. Conclusion

This study conducted a thorough examination of orchard trees through the classification of fruit trees according to distinct climatic zones, namely tropical, sub-tropical, and temperate. The study analyzed a total of 22 journals indexed in the Web of Science database and reviewed 74 articles within these journals.

The current review provides an in-depth analysis of the methods used in the past to identify orchard trees and define their crowns. For sure, efficient orchard management to support consistent and sufficient fruit yields was the ultimate goal. Efficient utilization of products from space-borne, airborne, and terrestrial systems can be facilitated by a range of conventional and modern digital image analysis techniques, which are dependent on the type of information being utilized. Deep learning techniques are the latest method utilized to reach this goal. In this context, it is noted that ongoing efforts to develop new methods and algorithms are improving the effectiveness of processes for identifying

and modeling fruit trees in orchards.

In the course of future research in this field, multiple aspects should be investigated. To improve the quality of the input data, multiple image acquisition variables, such as flying altitude, image side-lap, flying speed, flying directions, and solar elevation, must be carefully analyzed. Because having a diverse set of training data is always the key to high performance, the training dataset needs to be enriched with additional types of data before any further modeling research can be conducted. For larger areas, more accurate and time-efficient methods of acquiring information about fruit trees should be developed, and potential future studies could focus on orchards that contain a wide variety of fruit tree species. If the models of fruit trees can be embedded in a digital framework, then they can be used for online yield estimation as well as precision agriculture. Open-source cloud platforms can also meet the need to share data and iterate on parameters for global areas to standardize the workflows developed.

Declaration of Competing Interest

The authors declare that they have no known competing financial interests or personal relationships that could have appeared to influence the work reported in this paper.

Data availability

No data was used for the research described in the article.

References

- Aksoy, S., Yalniz, I.Z., Tasdemir, K., 2012. Automatic detection and segmentation of orchards using very high resolution imagery. *IEEE Trans. Geosci. Remote Sens.* 50, 3117–3131. <https://doi.org/10.1109/TGRS.2011.2180912>.
- Alonso, L., Picos, J., Bastos, G., Armesto, J., 2020. Detection of very small tree plantations and tree-level characterization using open-access remote-sensing databases. *Remote Sens. (Basel)* 12, 2276. <https://doi.org/10.3390/rs12142276>.
- Blekots, K., Tsakas, A., Xouris, C., Evdokidis, I., Alexandropoulos, D., Alexakos, C., Katakis, S., Makedonas, A., Theoharatos, C., Lalos, A., 2021. Analysis, modeling and multi-spectral sensing for the predictive management of verticillium wilt in olive groves. *JSAN* 10, 15. <https://doi.org/10.3390/jsan10010015>.
- Calderón, R., Navas-Cortés, J., Zarco-Tejada, P., 2015. Early detection and quantification of verticillium wilt in olive using hyperspectral and thermal imagery over large areas. *Remote Sens.* 7, 5584–5610. <https://doi.org/10.3390/rs70505584>.
- Camino, C., Zarco-Tejada, P., Gonzalez-Dugo, V., 2018. Effects of heterogeneity within tree crowns on airborne-quantified SIF and the CWSI as indicators of water stress in the context of precision agriculture. *Remote Sens. (Basel)* 10, 604. <https://doi.org/10.3390/rs10040604>.
- Chen, Y., Hou, C., Tang, Y., Zhuang, J., Lin, J., He, Y., Guo, Q., Zhong, Z., Lei, H., Luo, S., 2019. Citrus tree segmentation from UAV images based on monocular machine vision in a natural orchard environment. *Sensors* 19, 5558. <https://doi.org/10.3390/s19245558>.
- Ciriza, R., Sola, I., Albizu, L., Álvarez-Mozos, J., González-Audicana, M., 2017. Automatic detection of uprooted orchards based on orthophoto texture analysis. *Remote Sens. (Basel)* 9, 492. <https://doi.org/10.3390/rs9050492>.
- Çilliik, O., Cherbini, J., Johnson, R., Lyons, A., Kelly, M., 2018. Identification of citrus trees from unmanned aerial vehicle imagery using convolutional neural networks. *Drones* 2, 39. <https://doi.org/10.3390/drones2040039>.
- Dale, A., Galic, D., Leuty, T., Filotas, M., Currie, E., 2012. Hazelnuts in ontario — biology and potential varieties. *Fact Sheet, Order 240 no12-007Agdex*.
- Di Gennaro, S.F., Nati, C., Dainelli, R., Pastonchi, L., Berton, A., Toscano, P., Matese, A., 2020. An automatic UAV based segmentation approach for pruning biomass estimation in irregularly spaced chestnut orchards. *Forests* 11, 308. <https://doi.org/10.3390/f11030308>.
- Dong, X., Zhang, Z., Yu, R., Tian, Q., Zhu, X., 2020. Extraction of information about individual trees from high-spatial-resolution UAV-acquired images of an orchard. *Remote Sens. (Basel)* 12, 133. <https://doi.org/10.3390/rs12010133>.
- Dommez, C., Villi, O., Berberoglu, S., Cilek, A., 2021. Computer vision-based citrus tree detection in a cultivated environment using UAV imagery. *Comput. Electron. Agric.* 187, 106273. <https://doi.org/10.1016/j.compag.2021.106273>.
- Estornell, J., Velázquez-Martí, B., López-Cortés, I., Salazar, D., Fernández-Sarría, A., 2014. Estimation of wood volume and height of olive tree plantations using airborne discrete-return LiDAR data. *Gisci. Remote Sens.* 51, 17–29. <https://doi.org/10.1080/15481603.2014.883209>.
- FAO Statistics, 2019. *World Food and Agriculture Statistical PocketBook. Food and Agriculture Organization of the United Nations Rome*.
- Fieber, K.D., Davenport, I.J., Ferryman, J.M., Gurney, R.J., Walker, J.P., Hacker, J.M., 2013. Analysis of full-waveform LiDAR data for classification of an orange orchard scene. *ISPRS J. Photogramm. Remote Sens.* 82, 63–82. <https://doi.org/10.1016/j.isprsjprs.2013.05.002>.
- Friedl, M.A., Brodley, C.E., 1997. Decision tree classification of land cover from remotely sensed data. *Remote Sens. Environ.* 61, 399–409. [https://doi.org/10.1016/S0034-4257\(97\)00049-7](https://doi.org/10.1016/S0034-4257(97)00049-7).
- Gómez, J.A., Zarco-Tejada, P.J., García-Morillo, J., Gama, J., Soriano, M.A., 2011. Determining biophysical parameters for olive trees using CASI-airborne and quickbird-satellite imagery. *Agron. J.* 103, 644–654. <https://doi.org/10.2134/agronj2010.0449>.
- García-Murillo, D.G., Caicedo-Acosta, J., Castellanos-Dominguez, G., 2020. Individual detection of citrus and avocado trees using extended maxima transform summation on digital surface models. *Remote Sens. (Basel.)* 12, 1633. <https://doi.org/10.3390/rs12101633>.
- Gomes, M.F., Maillard, P., 2016. Detection of tree crowns in very high spatial resolution images. In: Marghany, M. (Ed.). *Environmental Applications of Remote Sensing*. InTech. <https://doi.org/10.5772/62122>.
- Gomes, M.F., Maillard, P., Deng, H., 2018. Individual tree crown detection in sub-meter satellite imagery using Marked Point Processes and a geometrical-optical model. *Remote Sens. Environ.* 211, 184–195. <https://doi.org/10.1016/j.rse.2018.04.002>.
- Hadas, E., Borkowski, A., Estornell, J., Tymkow, P., 2017. Automatic estimation of olive tree dendrometric parameters based on airborne laser scanning data using alpha-shape and principal component analysis. *Gisci. Remote Sens.* 54, 898–917. <https://doi.org/10.1080/15481603.2017.1351148>.
- Hadas, E., Jozkow, G., Walicka, A., Borkowski, A., 2019. Apple orchard inventory with a LiDAR equipped unmanned aerial system. *Int. J. Appl. Earth Observ. Geoinform.* 82, 101911. <https://doi.org/10.1016/j.jag.2019.101911>.
- Hobart, M., Pfanzl, M., Weltzien, C., Schirrmann, M., 2020. Growth height determination of tree walls for precise monitoring in apple fruit production using UAV photogrammetry. *Remote Sens. (Basel.)* 12, 1656. <https://doi.org/10.3390/rs12101656>.
- Hu, J., Zhang, Y., Zhao, D., Yang, G., Chen, F., Zhou, C., Chen, W., 2022. A robust deep learning approach for the quantitative characterization and clustering of peach tree crowns based on UAV images. *IEEE Trans. Geosci. Remote Sens.* 60, 1–13. <https://doi.org/10.1109/TGRS.2022.3142288>.
- Hu, L., Xu, X., Wang, J., Xu, H., 2023. Individual tree crown width detection from unmanned aerial vehicle images using a revised local transect method. *Ecol. Inform.* 75, 102086. <https://doi.org/10.1016/j.ecoinf.2023.102086>.
- Illana Rico, S., Martínez Gila, D.M., Cano Marchal, P., Gómez Ortega, J., 2022. Automatic detection of olive tree canopies for groves with thick plant cover on the ground. *Sensors* 22, 6219. <https://doi.org/10.3390/s22166219>.
- Jang, J.-D., Payan, V., Viau, A.A., Devost, A., 2008. The use of airborne lidar for orchard tree inventory. *Int. J. Remote Sens.* 29, 1767–1780. <https://doi.org/10.1080/01431160600928591>.
- Jiménez-Brenes, F.M., López-Granados, F., De Castro, A.I., Torres-Sánchez, J., Serrano, N., Peña, J.M., 2017. Quantifying pruning impacts on olive tree architecture and annual canopy growth by using UAV-based 3D modelling. *Plant Methods* 13, 55. <https://doi.org/10.1186/s13007-017-0205-3>.
- Johansen, K., Raharjo, T., McCabe, M., 2018. Using multi-spectral UAV imagery to extract tree crop structural properties and assess pruning effects. *Remote Sens. (Basel.)* 10, 854. <https://doi.org/10.3390/rs10060854>.
- Jurado, J.M., Ortega, L., Cubillas, J.J., Feito, F.R., 2020. Multispectral mapping on 3D models and multi-temporal monitoring for individual characterization of olive trees. *Remote Sens. (Basel.)* 12, 1106. <https://doi.org/10.3390/rs12071106>.
- Kawashita Kobayashi, F., Britto Mattos, A., Gemignani, B.H., Macedo, M.M.G., 2019. Experimental Analysis of Citrus Tree Classification from UAV Images. *IEEE, San Diego, CA, USA*, pp. 32–327. <https://doi.org/10.1109/ISM46123.2019.00014>.
- Ke, Y., Quackenbush, L.J., 2011. A comparison of three methods for automatic tree crown detection and delineation from high spatial resolution imagery. *Int. J. Remote Sens.* 32, 3625–3647. <https://doi.org/10.1080/01431161003762355>.
- Kestur, R., Angural, A., Bashir, B., Omkar, S.N., Anand, G., Meenavathi, M.B., 2018. Tree crown detection, delineation and counting in UAV remote sensed images: a neural network based spectral-spatial method. *J. Indian Soc. Remote Sens.* 46, 991–1004. <https://doi.org/10.1007/s12524-018-0756-4>.
- Kia, S., 2019. Individual tree delineation from high resolution Sar image using the scale-space blob method. *Thesis in Master of Science in Geo-information Science and Earth Observation. University of Twente, Enschede, The Netherlands*.
- Koc-San, D., Selim, S., Aslan, N., San, B.T., 2018. Automatic citrus tree extraction from UAV images and digital surface models using circular Hough transform. *Comput. Electron. Agric.* 150, 289–301. <https://doi.org/10.1016/j.compag.2018.05.001>.
- Kozhoridze, G., Orlovsky, N., Orlovsky, L., Blumberg, D.G., Golani-Goldhirsh, A., 2018. Classification-based mapping of trees in commercial orchards and natural forests. *Int. J. Remote Sens.* 39, 8784–8797. <https://doi.org/10.1080/01431161.2018.1492178>.
- López-Granados, F., Torres-Sánchez, J., Jiménez-Brenes, F.M., Arquero, O., Lovera, M., De Castro, A.I., 2019. An efficient RGB-UAV-based platform for field almond tree phenotyping: 3-D architecture and flowering traits. *Plant Methods* 15, 160. <https://doi.org/10.1186/s13007-019-0547-0>.
- Lin, C., Jin, Z., Mulla, D., Ghosh, R., Guan, K., Kumar, V., Cai, Y., 2021. Toward large-scale mapping of tree crops with high-resolution satellite imagery and deep learning algorithms: a case study of olive orchards in morocco. *Remote Sens. (Basel.)* 13, 1740. <https://doi.org/10.3390/rs13091740>.
- Liu, Z., Guo, P., Liu, H., Fan, P., Zeng, P., Liu, X., Feng, C., Wang, W., Yang, F., 2021. Gradient boosting estimation of the leaf area index of apple orchards in UAV remote sensing. *Remote Sens.* 13, 3263. <https://doi.org/10.3390/rs13163263>.

- Mahour, M., Tolpekin, V., Stein, A., 2020. Automatic detection of individual trees from VHR satellite images using scale-space methods. *Sensors* 20, 7194. <https://doi.org/10.3390/s20247194>.
- Marques, P., Pádua, L., Adão, T., Hruška, J., Peres, E., Sousa, A., Sousa, J.J., 2019. UAV-based automatic detection and monitoring of chestnut trees. *Remote Sens. (Basel)* 11, 855. <https://doi.org/10.3390/rs11070855>.
- Martínez-Casasnovas, J.A., Sandomí-Pozo, L., Escolà, A., Arnó, J., Llorens, J., 2022. Delineation of management zones in hedgerow almond orchards based on vegetation indices from UAV images validated by LiDAR-derived canopy parameters. *Agronomy* 12, 102. <https://doi.org/10.3390/agronomy12010102>.
- Mohapatra, D., Mishra, S., Giri, S., Kar, A., 2013. Application of hurdles for extending the shelf life of fresh fruits. *Trends in Post-Harvest Technol.* 1, 37–54.
- Mu, Y., Fujii, Y., Takata, D., Zheng, B., Noshita, K., Honda, K., Ninomiya, S., Guo, W., 2018. Characterization of peach tree crown by using high-resolution images from an unmanned aerial vehicle. *Hortic. Res.* 5, 74. <https://doi.org/10.1038/s41438-018-0097-z>.
- Murray, J., Fennell, J.T., Blackburn, G.A., Whyatt, J.D., Li, B., 2020. The novel use of proximal photogrammetry and terrestrial LiDAR to quantify the structural complexity of orchard trees. *Precision Agric.* 21, 473–483. <https://doi.org/10.1007/s11119-019-09676-4>.
- Niccolai, A., Hohl, A., Niccolai, M., Oliver, C.D., 2010. Integration of varying spatial, spectral and temporal high-resolution optical images for individual tree crown isolation. *Int. J. Remote Sens.* 31, 5061–5088. <https://doi.org/10.1080/014311609093283850>.
- Ok, A.O., Ozdarici-Ok, A., 2018a. 2-D delineation of individual citrus trees from UAV-based dense photogrammetric surface models. *Int. J. Digit. Earth* 11, 583–608. <https://doi.org/10.1080/17538947.2017.1337820>.
- Ok, A.O., Ozdarici-Ok, A., 2018b. Combining orientation symmetry and LM cues for the detection of citrus trees in orchards from a digital surface model. *IEEE Geosci. Remote Sens. Lett.* 15, 1817–1821. <https://doi.org/10.1109/LGRS.2018.2865003>.
- Ok, A.O., Ozdarici-Ok, A., Baseski, E., 2018. Accuracy assessment of pleiades-1 Stereo/Tri-stereos digital surface models: a case study for citrus trees. *J. Indian Soc. Remote Sens.* 46, 1203–1212. <https://doi.org/10.1007/s12524-018-0809-8>.
- Oscio, L.P., Arruda, M.D.S.D., Marcato Junior, J., Da Silva, N.B., Ramos, A.P.M., Moryia, É.A.S., Imai, N.N., Pereira, D.R., Creste, J.E., Matsubara, E.T., Li, J., Gonçalves, W.N., 2020. A convolutional neural network approach for counting and geolocating citrus-trees in UAV multispectral imagery. *ISPRS J. Photogram. Remote Sens.* 160, 97–106. <https://doi.org/10.1016/j.isprsjprs.2019.12.010>.
- Oscio, L.P., Nogueira, K., Marques Ramos, A.P., Faith Pinheiro, M.M., Furuya, D.E.G., Gonçalves, W.N., De Castro Jorge, L.A., Marcato Junior, J., Dos Santos, J.A., 2021. Semantic segmentation of citrus-orchard using deep neural networks and multispectral UAV-based imagery. *Precision Agric.* 22, 1171–1188. <https://doi.org/10.1007/s11119-020-09777-5>.
- Ottroy, S., Tziolas, N., Van Meerbeek, K., Aravidis, I., Tilkin, S., Sismanis, M., Stavrakoudis, D., Gitas, I.Z., Zalidis, G., De Vocht, A., 2022. Effects of flight and smoothing parameters on the detection of taxus and olive trees with UAV-borne imagery. *Drones* 6, 197. <https://doi.org/10.3390/drones6080197>.
- Ozdarici-Ok, A., 2015. Automatic detection and delineation of citrus trees from VHR satellite imagery. *Int. J. Remote Sens.* 36, 4275–4296. <https://doi.org/10.1080/01431161.2015.1079663>.
- Özcan, A.H., Hisar, D., Sayar, Y., Ünsalan, C., 2017. Tree crown detection and delineation in satellite images using probabilistic voting. *Remote Sens. Lett.* 8, 761–770. <https://doi.org/10.1080/2150704X.2017.1322733>.
- Pádua, L., Vanko, J., Hruška, J., Adão, T., Sousa, J.J., Peres, E., Morais, R., 2017. UAS, sensors, and data processing in agroforestry: a review towards practical applications. *Int. J. Remote Sens.* 38, 2349–2391. <https://doi.org/10.1080/01431161.2017.1297548>.
- Panda, S.S., Hoogenboom, G., Paz, J.O., 2010. Remote sensing and geospatial technological applications for site-specific management of fruit and Nut Crops: a review. *Remote Sens. (Basel)* 2, 1973–1997. <https://doi.org/10.3390/rs2081973>.
- Pforte, F., Selbeck, J., Hensel, O., 2012. Comparison of two different measurement techniques for automated determination of plum tree canopy cover. *Biosyst. Eng.* 113, 325–333. <https://doi.org/10.1016/j.biosystemseng.2012.09.014>.
- Pleșoianu, A.-I., Stupariu, M.-S., Șandric, I., Pătru-Stupariu, I., Drăguț, L., 2020. Individual tree-crown detection and species classification in very high-resolution remote sensing imagery using a deep learning ensemble model. *Remote Sens. (Basel)* 12, 2426. <https://doi.org/10.3390/rs12152426>.
- Ponce, J.M., Aquino, A., Tejada, D., Al-Hadithi, B.M., Andújar, J.M., 2022. A methodology for the automated delineation of crop tree crowns from UAV-based aerial imagery by means of morphological image analysis. *Agronomy* 12, 43. <https://doi.org/10.3390/agronomy12010043>.
- Recio, J.A., Hermosilla, T., Ruiz, L.A., Palomar, J., 2013. Automated extraction of tree and plot-based parameters in citrus orchards from aerial images. *Comput. Electron. Agric.* 90, 24–34. <https://doi.org/10.1016/j.compag.2012.10.005>.
- Reis, S., Taşdemir, K., 2011. Identification of hazelnut fields using spectral and Gabor textural features. *ISPRS J. Photogram. Remote Sens.* 66, 652–661. <https://doi.org/10.1016/j.isprsjprs.2011.04.006>.
- Santoro, F., Tarantino, E., Figorito, B., Gualano, S., D’Onghia, A.M., 2013. A tree counting algorithm for precision agriculture tasks. *Int. J. Digital Earth* 6, 94–102. <https://doi.org/10.1080/17538947.2011.642902>.
- Sarron, J., Malézieux, É., Sané, C., Faye, É., 2018. Mango yield mapping at the orchard scale based on tree structure and land cover assessed by UAV. *Remote Sens. (Basel)* 10, 1900. <https://doi.org/10.3390/rs10121900>.
- Solano, F., Di Fazio, S., Modica, G., 2019. A methodology based on GEOBIA and WorldView-3 imagery to derive vegetation indices at tree crown detail in olive orchards. *Int. J. Appl. Earth Observ. Geoinform.* 83, 101912. <https://doi.org/10.1016/j.jag.2019.101912>.
- Stateras, D., Kalivas, D., 2020. Assessment of olive tree canopy characteristics and yield forecast model using high resolution UAV imagery. *Agriculture* 10, 385. <https://doi.org/10.3390/agriculture10090385>.
- Stein, M., Bargoti, S., Underwood, J., 2016. Image based mango fruit detection, localisation and yield estimation using multiple view geometry. *Sensors* 16, 1915. <https://doi.org/10.3390/s16111915>.
- Taşdemir, K., 2012. Exploiting spectral and spatial information for the identification of hazelnut fields using self-organizing maps. *Int. J. Remote Sens.* 33, 6239–6253. <https://doi.org/10.1080/01431161.2012.682659>.
- Tian, H., Fang, X., Lan, Y., Ma, C., Huang, H., Lu, X., Zhao, D., Liu, H., Zhang, Y., 2022. Extraction of citrus trees from UAV remote sensing imagery using YOLOv5s and coordinate transformation. *Remote Sens. (Basel)* 14, 4208. <https://doi.org/10.3390/rs14174208>.
- Torres-Sánchez, J., De Castro, A.I., Peña, J.M., Jiménez-Brenes, F.M., Arqueró, O., Lovera, M., López-Granados, F., 2018a. Mapping the 3D structure of almond trees using UAV acquired photogrammetric point clouds and object-based image analysis. *Biosyst. Eng.* 176, 172–184. <https://doi.org/10.1016/j.biosystemseng.2018.10.018>.
- Torres-Sánchez, J., López-Granados, F., Borrà-Serrano, I., Peña, J.M., 2018b. Assessing UAV-collected image overlap influence on computation time and digital surface model accuracy in olive orchards. *Precision Agric.* 19, 115–133. <https://doi.org/10.1007/s11119-017-9502-0>.
- Tu, Y.-H., Phinn, S., Johansen, K., Robson, A., Wu, D., 2020. Optimising drone flight planning for measuring horticultural tree crop structure. *ISPRS J. Photogram.* *Remote Sens.* 160, 83–96. <https://doi.org/10.1016/j.isprsjprs.2019.12.006>.
- Underwood, J.P., Hung, C., Whelan, B., Sukkarieh, S., 2016. Mapping almond orchard canopy volume, flowers, fruit and yield using lidar and vision sensors. *Comput. Electron. Agric.* 130, 83–96. <https://doi.org/10.1016/j.compag.2016.09.014>.
- Vahidi, H., Klinkenberg, B., Johnson, B., Moskal, L., Yan, W., 2018. Mapping the individual trees in urban orchards by incorporating volunteered geographic information and very high resolution optical remotely sensed data: a template matching-based approach. *Remote Sens. (Basel)* 10, 1134. <https://doi.org/10.3390/rs10071134>.
- Vinci, A., Brigante, R., Traini, C., Farinelli, D., 2023. Geometrical characterization of hazelnut trees in an intensive orchard by an unmanned aerial vehicle (UAV) for precision agriculture applications. *Remote Sens. (Basel)* 15, 541. <https://doi.org/10.3390/rs15020541>.
- Wu, J., Yang, G., Yang, H., Zhu, Y., Li, Z., Lei, L., Zhao, C., 2020. Extracting apple tree crown information from remote imagery using deep learning. *Comput. Electron. Agric.* 174, 105504. <https://doi.org/10.1016/j.compag.2020.105504>.
- Yandutín Narváez, F.J., Salvo Del Pedregal, J., Prieto, P.A., Torres-Torriti, M., Auat Cheein, F.A., 2016. LiDAR and thermal images fusion for ground-based 3D characterisation of fruit trees. *Biosyst. Eng.* 151, 479–494. <https://doi.org/10.1016/j.biosystemseng.2016.10.012>.
- Ye, Z., Wei, J., Lin, Y., Guo, Q., Zhang, J., Zhang, H., Deng, H., Yang, K., 2022. Extraction of olive crown based on UAV visible images and the U2-Net deep learning model. *Remote Sens. (Basel)* 14, 1523. <https://doi.org/10.3390/rs14061523>.
- Yuan, H., Huang, K., Ren, C., Xiong, Y., Duan, J., Yang, Z., 2022. Pomelo tree detection method based on attention mechanism and cross-layer feature fusion. *Remote Sens.* 14, 3902. <https://doi.org/10.3390/rs14163902>.
- Zhang, Z., Jin, Y., Chen, B., Brown, P., 2019. California almond yield prediction at the orchard level with a machine learning approach. *Front. Plant Sci.* 10, 809. <https://doi.org/10.3389/fpls.2019.00809>.
- Zhao, H., Morgenroth, J., Pearse, G., Schindler, J., 2023. A systematic review of individual tree crown detection and delineation with convolutional neural networks (CNN). *Curr. Forestry Rep.* <https://doi.org/10.1007/s40725-023-00184-3>.
- Zhu, Y., Zhou, J., Yang, Y., Liu, L., Liu, F., Kong, W., 2022. Rapid target detection of fruit trees using UAV imaging and improved light YOLOv4 algorithm. *Remote Sens. (Basel)* 14, 4324. <https://doi.org/10.3390/rs14174324>.